Volume 382, issue 2 15 August 2007 ISSN 0378-4371

Available online at
ScienceDirect
www.sciencedirect.com
http://www.elsevier.com/locate/physa

Available online at www.sciencedirect.com
ScienceDirect
Physica A 382 (2007) 597–615
PHYSICA A
www.elsevier.com/locate/physa

The elliptical dimension of space-time atmospheric stratification of passive admixtures using lidar data

A. Radkevich[a], S. Lovejoy[a,*], K. Strawbridge[b], D. Schertzer[c,d]

[a]*Department of Physics, McGill University, 3600 University St. Montreal, QC, Canada H3A 2T8*
[b]*Science and Technology Branch, Environment Canada, Centre for Atmospheric Research Experiments, 6248 Eight Line, Egbert, ON, Canada, L0L 1N0*
[c]*CEREVE, Ecole Nationale des Ponts et Chaussées, 6-8, Ave. Blaise Pascal, Cité Descartes, 77455 Marne-la-Valleé, Cedex 2, France*
[d]*Météo France, 1 Quai Branly, Paris, 75007, France*

Received 25 April 2006; received in revised form 16 February 2007
Available online 3 April 2007

Abstract

State-of-the-art airborne lidar data of passive scalars have shown that the spatial stratification of the atmosphere is scaling: the vertical extent (Δz) of structures is typically $\approx \Delta x^{H_z}$ where Δx is the horizontal extent and H_z is a stratification exponent. Assuming horizontal isotropy, the volumes of the structures therefore vary as $\Delta x \Delta x \Delta x^{H_z} = \Delta x^{D_s}$ where the "elliptical dimension" D_s characterizes the rate at which the volumes of typical non-intermittent structures vary with scale. Work on vertical cross-sections has shown that $2 + H_z = 2.55 \pm 0.02$ (close to the theoretical prediction 23/9).

In this paper we extend these (x, z) analyses to (z, t). In the absence of overall advection, the lifetime Δt of a structure of size Δx varies as Δx^{H_t} with $H_t = 2/3$ so that the overall space-time dimension is $D_{st} = 29/9 = 3.22\ldots$. However, horizontal and vertical advection lead to new exponents: we argue that the temporal stratification exponent $H_t \approx 1$ or ≈ 0.7 depending on the relative importance of horizontal versus vertical advection velocities. We empirically test these space-time predictions using vertical-time (z, t) cross-sections using passive scalar surrogates (aerosol backscatter ratios from lidar) at ~3 m resolution in the vertical, 0.5–30 s in time and spanning 3–4 orders of magnitude in scale as well as new analyses of vertical (x, z) cross-sections (spanning over 3 orders of magnitude in both x, z directions). In order to test the theory for density fluctuations at arbitrary displacements in (Δz, Δt) and (Δx, Δz) spaces, we developed and applied a new Anisotropic Scaling Analysis Technique (ASAT) based on nonlinear coordinate transformations. Applying this and other analyses to data spanning more than 3 orders of magnitude of space-time scales we determined the anisotropic scaling of space-time finding the empirical value $D_{st} = 3.13 \pm 0.16$. The analyses also show that both cirrus clouds and aerosols had very similar space-time scaling properties. We point out that this model is compatible with (nonlinear) "turbulence" waves, hence potentially explaining the observed atmospheric structures.

Keywords: Stratification; Turbulence; Multifractals; Scaling; Atmospheric structure; Passive scalars

*Corresponding author. Tel.: +1 514 3986537; fax: +1 514 3988434.
E-mail address: lovejoy@physics.mcgill.ca (S. Lovejoy).

0378-4371/$ - see front matter © 2007 Elsevier B.V. All rights reserved.
doi:10.1016/j.physa.2007.03.046

1. Introduction

A fundamental aspect of atmospheric turbulence is its spatial anisotropy, in particular its vertical stratification associated with gravity. Even the most recent progress achieved in studying anisotropy in (gravity free) incompressible Navier–Stokes turbulence [1–5] (see below), does not solve the fundamental deficiencies of the ageing but still mainstream model of (gravity induced) atmospheric stratification. This model postulates a superposition of small-scale isotropic 3-D and large-scale isotropic 2-D turbulence separated by an "energy mesoscale gap" somewhere near the meso-scale (~10 km). It was theoretically and empirically shown that these deficiencies called for a drastic change of the notion of scaling [6,7], i.e. to first postulate the relevance of scaling, then study the resulting symmetries, instead of the classical approach that first postulates isotropy.

Several arguments favour this new anisotropic picture. First, the postulated energy gap which was expected to be a sharp "dimensional transition" between the 3-D and 2-D regimes, had no compelling empirical support whereas it is indispensable in preventing the small scale 3-D regime from destabilizing the large scale 2-D regime [8]. Second—in spite of many proposals—it is still not clear how to plausibly distribute the various sources and sinks of energy and enstrophy. Third, the assumption that any atmospheric turbulent regime might be isotropic, seems rather academic since gravity acts at all scales, not only at the meso-scale. As a consequence, over the last 20 years, most of the scientific community involved in statistical analysis of atmospheric stratification data have gradually opted for (strongly anisotropic) scaling stratification models in which there is no 2-D/3-D transition (scale break) and which has different spectral exponents in the horizontal and vertical directions.

A first approach [6] was to consider a turbulence whose horizontal wind (v) simultaneously displays different horizontal and vertical scaling laws for the velocity difference (fluctuation) Δv for, respectively, horizontal (Δx) and vertical (Δz) displacements: $\Delta v \propto \Delta x^{H_h}$, $\Delta v \propto \Delta z^{H_v}$ with distinct scaling horizontal (H_h) and vertical (H_v) exponents. In this framework, an eddy of a given horizontal gradient Δv, has typical horizontal extent Δx and vertical extent Δz; i.e. its size satisfies $\Delta z = \Delta x^{Hz}$; where $H_z = H_h/H_v$. We now see that if $H_v > H_h$ then $H_z < 1$ and that, therefore, the aspect ratio $\Delta z/\Delta x \propto \Delta x^{H_z-1}$ decreases with increasing Δx implying that structures become progressively flatter at larger and larger scales in a scaling manner. If we now assume horizontal isotropy so that the area of horizontal cross-sections is of the order Δx^2, then we see that the volume of structures varies as $\Delta x^2 \Delta x^{H_z} = \Delta x^{D_s}$ with $D_s = 2 + H_z$. Since the mean structures will typically be ellipsoids, D_s is called the "elliptical dimension" (the subscript "s" is for "spatial" to distinguish it from the space-time dimension D_{st} discussed below). Isotropic 3-D turbulence has $D_s = 3$, while isotropic 2-D turbulence (i.e. no vertical fluctuations) has $D_s = 2$, so that D_s characterizes the stratification. In terms of D_s, the mainstream model still favoured by atmospherists has a meso-scale transition from $D_s = 3$ to $D_s = 2$, whereas as discussed below, the turbulent buoyancy driven unified scaling model [7] has $D_s = 23/9$, while the quasi-linear gravity models have $D_s = 7/3$.

It is worth stressing that here and below, we are *not* discussing the much weaker anisotropies predicted for incompressible (gravity-free) Navier–Stokes turbulence [1–5,9] which predict that the wind velocity structure function is a sum of *isotropic* scaling laws i.e. with direction independent exponents (hence with $H_z = 1$, $D_s = 3$) i.e. with the effect of anisotropy confined to non-scaling prefactors. Some recent atmospheric experiments in the horizontal direction [1,3,4,9] determining the structure function of the horizontal wind have found some support for this approach for horizontal anisotropy—at least up to scales of several meters where the structure function would become negative.

Another approach to anisotropic turbulence involving isotropic scaling was proposed by Lumley [10]. Lumley considered shear flows with an imposed characteristic (shear) time scale. Using this to non-dimensionalize the turbulent eddy turn over time and making various smoothness and analyticity assumptions, he obtained a series expansion in terms of (isotropic) spectral corrections $k^{-7/3}$, $k^{-9/3}$ etc. (see also [11], for similar ideas in atmospheric boundary layer turbulence). Today, in the context of multifractal turbulence, these assumptions seem somewhat academic; see however [12].

A convenient way of distinguishing the theories of (gravity induced) stratification is thus to measure D_s. This was first attempted using quite distinct horizontal (e.g. airplane) and vertical (balloon) measurements [7], in one case with near synchronous measurements [13,14]. Thanks to the advent of high-powered lidars with

logarithmic amplifiers it is now possible to directly measure vertical atmospheric cross sections over greater dynamic range and obtain much more convincing results. Indeed, at least for the lower atmosphere (<3–4 km) cross-sections with over three orders of magnitude in scale in vertical and horizontal directions have been obtained; analyses yield $H_h/H_v = H_z = 0.55 \pm 0.02$ hence $D_s = 2.55 \pm 0.02$ [15], hence giving strong empirical support for the 23/9 ($= 2.555\ldots D$) model.

The theoretical prediction $H_z = 5/9$ is the consequence of a horizontal Kolmogorov law: $\Delta v = \varepsilon^{1/3}\Delta x^{1/3}$ ($H_h = 1/3$) and vertical Bolgiano–Obukhov law: $\Delta v = \phi^{1/5}\Delta z^{3/5}$ ($H_v = 3/5$) where ε is the energy flux, $\phi = \Delta f^2/\tau$ is the buoyancy variance flux (units of distance^2/time^5; $\Delta f = g\Delta \log\theta$ is the buoyancy force increment across a layer thickness Δz, and τ is the time scale of the transfer); hence $H_z = 1/3/(3/5) = 5/9$. Using these two fluxes, by dimensional analysis, we obtain basic length and time scales:

$$l_s = \phi^{-3/4}\varepsilon^{5/4},\ \tau_s = \phi^{-1/2}\varepsilon^{1/2}, \tag{1}$$

where l_s is the "sphero scale", τ_s is the eddy turn over time at the sphero-scale (the "sphero-time"), see below. In the original (3-D isotropic) Bolgiano–Obukhov law, the length scale $\phi^{-3/4}\varepsilon^{5/4}$ was called the "Bolgiano scale" and was considered to be the outer scale of an isotropic 3-D Kolmogorov regime and simultaneously the inner scale of an isotropic 3-D buoyancy-dominated Bolgiano–Obukhov regime. However, in the stratified 23/9-D model ε, ϕ are important at all scales so that it is not a transition from one regime to another, it is rather the scale at which typical vertical and horizontal fluctuations are equal, hence at which structures will be more or less isotropic, whence the term "sphero-scale". Since ε and ϕ are highly intermittent (multifractal) fluxes appropriate statistics must be used to determine l_s; see [16] and discussion below.

Since the velocity field "advects itself", if it is spatially scaling, then it is also scaling in time (and hence in space-time); in the absence of an overall advection, the classical Kolmogorov result (essentially dimensional analysis) yields $\Delta v = \varepsilon^{1/2}\Delta t^{H_\tau}$ with the temporal exponent $H_\tau = 1/2$ [17,18]. This implies that space-time volumes scale as $\Delta x\Delta y\Delta z\Delta t \approx \Delta x^{1+1+H_z+H_t}$ with $H_t = H_h/H_t = (1/3)/(1/2) = 2/3$. However, when advection is considered, the temporal scaling has two additional regimes corresponding to horizontal wind domination and vertical wind domination. In this paper we examine this question empirically with the help of lidar data and the new ASAT technique.

2. The predictions of the unified scaling model

As discussed above, the unified scaling model for atmospheric turbulence initially postulates:

$$\begin{aligned}
\Delta v(\Delta x, 0, 0, 0) &= \varepsilon_{\Delta x}^{1/3}\Delta x^{1/3},\\
\Delta v(0, \Delta y, 0, 0) &= \varepsilon_{\Delta y}^{1/3}\Delta y^{1/3},\\
\Delta v(0, 0, \Delta z, 0) &= \phi_{\Delta z}^{1/5}\Delta z^{3/5},\\
\Delta v(0, 0, 0, \Delta t) &= \varepsilon_{\Delta t}^{1/2}\Delta t^{1/2},
\end{aligned} \tag{2}$$

where ε is the energy flux, ϕ is the buoyancy variance flux; the subscripts indicate the scale of the increments.

To extend this to an arbitrary space-time displacement $\Delta\underline{R} = (\Delta\underline{r}, \Delta t)$, $\Delta\underline{r} = (\Delta x, \Delta y, \Delta z)$, a "generalized scale" $[\![\Delta\underline{R}]\!]$ was introduced so as to be linear with respect to the contraction ratio λ (see mathematical details in Ref. [19]):

$$[\![T_\lambda \Delta\underline{R}]\!] = \lambda^{-1}[\![\Delta\underline{R}]\!] \tag{3}$$

where T_λ transforms vectors into vectors reduced by factors of λ in scale. Since T_λ is a one-parameter (semi-) group with respect to λ it is defined by a generator G:

$$T_\lambda = \lambda^{-G}. \tag{4}$$

This "Generalized Scale Invariance" (GSI [6]) is the basic framework for defining scale in anisotropic scaling systems. In the linear case, G is a matrix and the generalized scale is position independent. When G is the identity matrix, we have the usual isotropic, self-similar scale changes. In the case of "linear GSI", where G is a

diagonal matrix, the system is "self affine" and we obtain stratification along a coordinate axis. When G has off-diagonal elements we have differential rotation and stratification.

To unify horizontal, vertical and temporal turbulent fluctuations as described in Eq. (2), the simplest case, but not a generic case as discussed below, corresponds to:

$$G_{st} = \begin{pmatrix} G_s & 0 \\ 0 & H_t \end{pmatrix}; \quad G_s = \begin{pmatrix} 1 & 0 & 0 \\ 0 & 1 & 0 \\ 0 & 0 & H_z \end{pmatrix}; \quad \begin{matrix} H_z = (1/3)/(3/5) = 5/9, \\ H_t = (1/3)/(1/2) = 2/3, \end{matrix} \tag{5}$$

where the rows and columns correspond to the x, y, z and t directions, respectively, G_s is the matrix corresponding to the spatial part only; stratification exponents H_z, H_t are the ratios of the scaling exponent in the horizontal over the scaling exponents in the vertical and in time respectively. The general definitions of the elliptical dimensions characterizing the spatial and space-time anisotropies are respectively '$D_s = Trace\ G_s$ and $D_{st} = Trace\ \ G_{st} = D_s + H$. With the above dimensionally determined exponents we obtain $D_s = 23/9$, $D_{st} = 29/9$.

We now consider solutions of the scale Eq. (3); it is sufficient to consider diagonal G, non-diagonal G can be dealt with by linear transformations (as with advection, see below). In this case, we can make the following nonlinear transformation of variables:

$$\Delta x' = \Delta x; \quad \Delta y' = \Delta y; \quad \Delta z' = l_s \mathrm{sgn}(\Delta z)(|\Delta z|/l_s)^{1/H_z}; \quad \Delta t' = l_s \mathrm{sgn}(\Delta t)(|\Delta t|/\tau_s)^{1/H_t}. \tag{6a}$$

In this primed space, we may define:

$$|\,\underline{\Delta R'}\,| = \left[\Delta x'^2 + \Delta y'^2 + \Delta z'^2 + \Delta t'^2\right]^{1/2}, \ \widehat{\Delta R'} = \frac{\underline{\Delta R'}}{|\,\underline{\Delta R'}\,|}, \tag{6b}$$

where $|\,\underline{\Delta R'}\,|$ and $\widehat{\Delta R'}$ are the usual distances and direction vectors. Due to Eq. (3), we have: $[\![\, \lambda^{-I}\, \underline{\Delta R'}\,]\!] = \lambda^{-1}[\![\, \underline{\Delta R'}\,]\!]$ i.e. $[\![\, \underline{\Delta R'}\,]\!]$ satisfies Eq. (3) with $G = I$ (the identity) and therefore is the usual norm with a possibly direction dependent prefactor:

$$[\![\, \Delta\, \underline{R'}\,]\!] = \Theta(\widehat{\Delta\, \underline{R'}})|\Delta\, \underline{R'}\,|. \tag{7}$$

where $\Theta(\widehat{\Delta\, \underline{R'}})$ is a function of polar angle in the $\Delta\, \underline{R'}$ space and determines the "trivial" anisotropy. We therefore obtain (for diagonal G):

$$\begin{aligned} [\![\, \Delta\, \underline{R}\,]\!] &= [\![\, (\Delta x, \Delta y, \Delta z, \Delta t)\,]\!] = \Theta(\widehat{\Delta R'})[\![\, \Delta\, \underline{R}\,]\!]_{can}, \\ [\![\, \Delta\, \underline{R}\,]\!]_{can} &= |\Delta\, \underline{R'}\,| = l_s\left(\left(\frac{\Delta x}{l_s}\right)^2 + \left(\frac{\Delta y}{l_s}\right)^2 + \left(\frac{\Delta z}{l_s}\right)^{2/H_z} + \left(\frac{\Delta t}{\tau_s}\right)^{2/H_t}\right)^{1/2}, \end{aligned} \tag{8}$$

the subscript "*can*" for "canonical" indicates that $[\![\, \Delta\, \underline{R}\,]\!]_{can} = \left|\Delta\, \underline{R'}\right|$ is the simplest scale function (obtained with $\Theta = 1$). With the scale function $[\![\, \Delta\, \underline{R}\,]\!]$ the anisotropic Kolmogorov–Bolgiano–Obukhov law (2) can be written for arbitrary space-time displacement vectors:

$$\Delta v(\Delta\, \underline{R}) \approx \varepsilon_{[[\Delta\, \underline{R}]]}^{1/3}[\![\, \Delta\, \underline{R}\,]\!]^{1/3}. \tag{9}$$

If the scale function is indeed the appropriate turbulent notion of scale then it must be used in all the turbulence laws in the place of the (isotropic) vector norm. In this way, we obtain the anisotropic generalization of the Corrsin–Obukhov law:

$$\Delta\rho(\Delta\, \underline{R}) \approx \chi_{[[\Delta\, \underline{R}]]}^{1/2}\varepsilon_{[[\Delta\, \underline{R}]]}^{-1/6}[\![\, \Delta\, \underline{R}\,]\!]^{1/3}, \tag{10}$$

where χ is the passive scalar variance flux and $\Delta\rho$ is a fluctuation in the concentration of a passive scalar. Obviously, for $\underline{\Delta R} = (\Delta x, 0, 0, 0)$ we obtain the usual Corrsin–Obukhov law; however in the vertical with $\underline{\Delta R} = (0, 0, \Delta z, 0)$ we obtain the new law:

$$\Delta\rho(0, 0, \Delta z, 0) \approx \chi^{1/2}\varepsilon^{-1/2}\phi^{1/5}\Delta z^{3/5}. \tag{11}$$

In Ref. [15] both this and the standard horizontal $\Delta x^{1/3}$ law were well verified on passive scalar surrogates (pollution aerosols) using airborne lidar data from the lower 5 km of the atmosphere.

It is generally important to take into account the possible mean advection of the system. In order to handle advection, we only need to perform a Galilean transformation [20,21]:

$$G_{st} \to A^{-1} G_{st} A;\ [\![\Delta \underline{R}]\!] \to [\![A^{-1} \Delta \underline{R}]\!]; \quad A = \begin{pmatrix} 1 & 0 & 0 & u \\ 0 & 1 & 0 & v \\ 0 & 0 & 1 & w \\ 0 & 0 & 0 & 1 \end{pmatrix}, \tag{12}$$

where $\underline{V} = (u, v, w)$ is the advection velocity. The advection therefore introduces a non-diagonal generator. However, the relationship between the two Galilean frameworks is straightforward:

$$\underline{\Delta R''} = A^{-1}\, \underline{\Delta R}; \quad \begin{aligned} \Delta \underline{x}'' &= \Delta \underline{x} - \underline{V}\, \Delta t, \\ \Delta t'' &= \Delta t, \end{aligned} \tag{13}$$

hence:

$$[\![(\Delta x, \Delta y, \Delta z, \Delta t)]\!]_{\mathrm{adv}} = l_v \Theta(\widehat{\Delta R'}) \left(\left(\frac{\Delta x - u\Delta t}{l_s} \right)^2 + \left(\frac{\Delta y - v\Delta t}{l_s} \right)^2 + \left(\frac{\Delta z - w\Delta t}{l_s} \right)^{2/H_z} + \left(\frac{\Delta t}{\tau_s} \right)^{2/H_t} \right)^{1/2}, \tag{14}$$

where again $\Theta(\widehat{\underline{\Delta R'}})$ determines the "trivial" anisotropy, i.e. simply a function of polar angle in the $\underline{\Delta R'}$ space; below we empirically estimate both G and Θ. Note that advection does not change TrG_{st}; the elliptical dimension is unaffected.

Considering temporal statistics ($\Delta x = \Delta y = \Delta z = 0$), depending on l_s, τ_s determined by Eq. (1), and components of wind velocity, the radical in Eq. (14) involves three different types of time development with exponents of 2 (horizontal wind domination), $2/H_t = 3$ (pure temporal development or "time domination") and $2/H_z = 18/5$ (vertical wind domination). This leads to three critical times defined by the Δt's for which one term exceeds the other. In Ref. [16] these are investigated with the help of meteorological data. It was shown that the probability that the transition from horizontal wind domination to vertical wind domination occurs at time scales less than 10^2 s is ~5% while the same probability of transition from horizontal wind domination to time domination (according to Eq. (14)) is significant only at scales $\sim 10^5$ s i.e. close to the eddy turn-over time of the largest atmospheric eddies ($\sim 10^6$ s). This result is compatible with that of Tennekes [22] based on the argument that the effect due to the "sweeping" of the small eddies by the large ones that pure temporal development will not be observable at time scales smaller than the eddy turn-over time (lifetime) of the largest eddies, about 2 weeks in atmosphere.

Even if we do not expect to see pure temporal development, we must still consider more closely the scaling of the vertical velocity term (which meteorological analyses indicate can occasionally be dominant). Whereas it is more or less easy to define a non-zero horizontal mean advection (u, v) at large scale (e.g. by averaging the horizontal wind on that scale), this is rather different for the vertical wind, the vertical wind w is typically small and its mean value generally decreases approaching zero for large enough averaging scales, thus it appears on the contrary to be scale dependent. According to limited analysis of drop sonde data (which as with most measurement techniques have trouble estimating w), and meteorological analyses (which are also inaccurate), it appears that the spectrum of w is a power law $E_w(\omega) \sim \omega^{-\beta_\omega}$ with exponent $\beta_w < 1$. Indeed, it seems likely that the w field can be modeled by a fractional integration of order $H_w < 0$ of a conservative multifractal flux (this is thus a fractional differentiation, c.f. $H = 1/3$ for the usual Corrsin–Obukhov law). Ignoring intermittency corrections, this would yield $\beta_w = 1 + 2H_w < 1$. In the case $H_w < 0$, considering $\Delta x = \Delta y = \Delta z = 0$, the statistics are:

$$|(w)_{\Delta t}| = w_{L/l} \left(\frac{[\![\Delta t]\!]}{l} \right)^{H_w}; \quad [\![\Delta t]\!] = [\![(0, 0, 0, \Delta t)]\!] \tag{15}$$

(when $H_w > 0$ we need to use Δw in place of w in the above) and $(w)_{\Delta t}$ is the mean vertical velocity in the region size l over the time Δt; L is the outer scale of the variability. $w_{L/l}$ is the mean vertical wind over the domain size l

(i.e. over time scale $T>\Delta t$) so that the cascade has developed over the scale ratio L/l. Continuing to ignore intermittency we can roughly see the effect of the scaling Eq. (15): we obtain for $\Delta x=\Delta y=\Delta z=0$ $\Delta\rho\sim\Delta t^{(1+H_w)H/H_z}$ i.e. $H'_t=H_z/(1+H_w)$. We can now see that $H_w=-1/6$ implies $H'_t=H_t=2/3$. Taking into account intermittency and considering the scale function at a single point, and neglecting the horizontal wind (i.e. $u=v=0$) and pure temporal development terms (i.e. τ_s is large), we average over the vertical velocity fluctuations, and obtain [23]:

$$[\![\Delta t]\!]=l_s\left(\frac{\Delta t}{\tau'_s}\right)^{1/H'_t};\quad \tau'_s=\tau_s\left(\frac{v_s}{w_{L/l}}\right)\left(\frac{l}{l_s}\right)^{H_z-H'_t};\quad v_s=l_s/\tau_s, \tag{16}$$

where we have used the shorthand notation $[\![\Delta t]\!]=[\![(0,0,0,\Delta t)]\!]$ and H'_t depends on the statistics of w; with $H_w\approx-0.1$, we can readily have $H'_t\approx H_t$ [23] so that the vertical wind term can give an "effective" exponent very close to the pure temporal development exponent. v_s is the "sphero-velocity"; the typical horizontal velocity at the sphero-scale (typically of the order of mm/s). For large enough vertical velocities, τ'_s can be appreciably smaller than τ_s so that this velocity term with effective exponent H'_t can dominate the horizontal advection terms (i.e. $(\Delta t/\tau'_s)^{1/H'_t}>(\Delta t/\tau_s)^{1/H_t}$). Therefore, replacing $(\Delta t/\tau_s)^{1/H_t}$ with $(\Delta t/\tau'_s)^{1/H'_t}$ (and putting the "effective vertical velocity" to zero) we obtain the "effective scale function":

$$[\![\Delta\underline{R}]\!]_{advec,eff,can}=[\![A^{-1}\Delta\underline{R}]\!]_{eff,can}=l_s\left(\left(\frac{\Delta x-u\Delta t}{l_s}\right)^2+\left(\frac{\Delta y-v\Delta t}{l_s}\right)^2+\left(\frac{\Delta z}{l_s}\right)^{2/H_z}+\left(\frac{\Delta t}{\tau'_s}\right)^{2/H'_t}\right)^{1/2}. \tag{17}$$

This new scale function corresponds to an "effective generator" and effective advection matrix:

$$G_{st,eff}=\begin{pmatrix}1&0&0&0\\0&1&0&0\\0&0&H_z&0\\0&0&0&H'_t\end{pmatrix};\quad A_{eff}=\begin{pmatrix}1&0&0&u\\0&1&0&v\\0&0&1&0\\0&0&0&1\end{pmatrix}; \tag{18}$$

$$D_{st,eff,advec}=Tr(A_{eff}^{-1}G_{st,eff}A_{eff})=Tr(G_{st,eff})=2+H_z+H'_t. \tag{19}$$

We see that as long as $H'_t<1$ that this vertical wind term will eventually (at large enough Δt) dominate the horizontal wind. In the following, we primarily analyze times series of vertical profiles, i.e. we are most interested in the (z, t) domain. In addition, we did not observe any cases with a clear break in the temporal scaling, so we adopt an empirical view: in all cases where there is a single dominant temporal scaling term we expect the (z, t) scale function to have the following form:

$$[\![(\Delta z,\Delta t)]\!]_{advec,eff}=[\![(0,0,\Delta z,\Delta t)]\!]_{advec,eff}=\Theta(\theta)l_s\left(\left(\frac{\Delta t}{\tau_{s,eff}}\right)^2+\left(\frac{\Delta z}{l_s}\right)^{2/h}\right)^{1/(2H_{t,eff})}, \tag{20}$$

where $\Theta(\theta)$ is the trivial anisotropy prefactor, $h=H_{t,eff}/H_z$ and $H_{t,eff}$ is the exponent of the dominant temporal term equal to 1 for horizontal velocity, 2/3 for pure temporal development, H'_t for vertical wind dominance. The scale function can be rewritten in this way since its $H_{t,eff}$ power is symmetric with respect to the rescaled generator

$$G=\begin{pmatrix}h&0\\0&1\end{pmatrix} \tag{21}$$

in the $(\Delta z, \Delta t)$ domain. In this form, we seek to verify the above space–time scaling form and determine the value of h, which determines the stratification in the $(\Delta z, \Delta t)$ space.

Finally, we will need the corresponding equation in Fourier space obtained by Fourier transforming the second order moment (autocorrelation function):

$$P(k_z,\omega)\approx\tilde{\Theta}\langle\varphi_l^2\rangle[\![(k_z,\omega)]\!]^{-s}=\tilde{\Theta}\langle\varphi_L^2\rangle l_s^{-s}((k_zl_s)^{2/h}+(\omega\tau_s)^2)^{-s/2};\ s=D_{st}-2H-K_\varphi(2), \tag{22}$$

where $\varphi = \chi^{1/2}\varepsilon^{-1/6}$ and $D_{st} = Tr(G_{st})$ and $K_\varphi(2)$ is the intermittency correction; it is the scaling exponent of the variance of φ : $\langle \varphi_l^q \rangle \sim l^{-K_\varphi(q)}$. Where we have used the "generalized Tauberian theorem":

$$[\![(\Delta z, \Delta t)]\!]^H \underset{F.T.}{\leftrightarrow} [\![(k_z, \omega)]\!]^{-(D_{st}-H)}, \tag{23}$$

where "F.T." indicates Fourier transform. $\tilde{\Theta}$ is the Fourier trivial anisotropy function (whose argument is the angle in Fourier space), and Fourier scale function is symmetric with respect to G^T rather than G. Integrating out respectively k_z and ω to obtain the 1-D spectra, we obtain:

$$\begin{aligned} &E(k_z) \sim k_z^{-\beta_v}; \quad s > H_{t,eff}; \quad \beta_v = (H_{t,eff}/H_z)(s/H_{t,eff} - 1), \\ &E(\omega) \sim \omega^{-\beta_\tau}; \quad s > H_z; \quad \beta_\tau = (H_z/H_{t,eff})(s/H_z - 1). \end{aligned} \tag{24}$$

This allows us to obtain the exponent s in terms of the 1-D spectral exponents. Solving for s, we obtain: $s = \beta_\tau H_{t,eff} + H_z = \beta_v H_z + H_{t,eff}$ which leads to the useful relation: $(\beta_v - 1)/(\beta_\tau - 1) = H_{t,eff}/H_z = h$. Using the values, $\beta_\tau \approx 2$, $H_{t,eff} \approx 0.66$ in the case of vertical wind domination, we obtain $s \sim 1.88$ and using $\beta_\tau = 5/3$ and $H_{t,eff} = 1$ in the case of horizontal wind domination we obtain $s = \beta_\tau H_{t,eff} + H_z = 20/9$.

3. An overview of existing empirical evidence for temporal scaling

Eqs. (8,9) show that (ignoring intermittency corrections) temporal fluctuations can be of the scaling form $\Delta v \approx \Delta t^{H_\tau}$ with H_τ depending on the time scales and the strengths of the horizontal and vertical winds. As mentioned above, taking into account the temporal scaling of the vertical wind we saw that it leads to H'_t close to H_t so that we expect $H_\tau = 1/3$, 0.5 as the two possible exponents. Note that the corresponding (non-intermittent) spectral exponents are given by $\beta_\tau = 1 + 2H_\tau$ so that this leads to the values $\beta_\tau \sim 5/3$, 2.0. In the atmosphere, experiments commonly find $\beta_\tau \approx 5/3$ indicating that the horizontal wind is frequently large enough to be dominant (at least at small lags); although several authors have found $\beta_\tau \approx 2$ over wide ranges of altitudes and conditions [24–27]. If we concentrate on the temporal spectrum of passive scalars and wind measurements made from remote sensing of passive scalars (which are directly relevant to our lidar measurements below), we find that radar and lidar measurements yield $\beta_\tau \approx 5/3$ and 2 in lower atmosphere (troposphere and stratosphere) [24–28] middle [29] and upper middle atmosphere including Na layer (up to altitudes about of 110 km) [28,30–33]. Most of these experiments cover temporal scale ranges of factors of 10^3 or larger and collectively cover the range 1 min to 100 days.

Since the spatial and temporal scaling of atmospheric fields are dimensionally related by a velocity, if we assume that the latter is the turbulent wind then we expect the fields to share the same G matrix, hence same ratio of horizontal to vertical scaling exponents: $H_t = H_h/H_\tau \approx 0.7$ (low horizontal wind and/or significant horizontal wind but scaling vertical wind) or $H_t = 1$ (horizontal wind domination, i.e. $H_\tau = H_h$). A good source of data for this purpose is from precipitation; for example a limited lidar data study of precipitation by Lovejoy and Schertzer [34], found $H_t = 0.5 \pm 0.2$. More recently a much larger radar database studied by Venugopal et al. [35] found similar results (c.f. their "dynamic scaling exponent" $z = H_t$, which they found in 5 storms to be 0.66 ± 0.09 and in a sixth to be 1.2 ± 0.1; all are roughly compatible with $H_t = 2/3$ or $H_t = 1$).

In the laboratory, the relatively abundant high Reynolds numbers shear driven flows give the velocity dominant exponent $\beta_\tau \approx 5/3$. A more interesting comparison is with convective turbulence (e.g. Raleigh–Benard) experiments, which have no large scale forcing velocity and thus may allow us to observe $\beta_\tau \approx 2$. At present, the empirical situation is not clear because of the typical small range of scales in the scaling regime (often over only one or two octaves in scale see e.g. [36,37]). Indeed, in order to get around the poor scaling, it has become common to use extended self-similarity (see e.g. [36]) but this only allows the estimate of the relative scaling exponents (e.g. structure functions of different orders vs. second order structure function), not the absolute values we require here. The papers with the widest ranges (factors of ≈ 10) are [38,39] both of whose results are compatible with theoretical temporal exponent $\beta_\tau \approx 2$.

We thus see that overall, the existing data are compatible with the anisotropic scaling model, but that the status of the $\beta_\tau \approx 2$ exponent in particular is not well established.

4. The experiments

We seek to verify the anisotropic space-time scaling using Eq. (22) and ground-based upward pointing lidar data of passive scatter backscatter ratio (B). We used data from both airborne lidar (Environment Canada's AERosol Imaging Airborne Lidar—AERIAL [40] and ground-based lidar systems (mobile and fixed) operated out of the CARE facility in Egbert, Ontario. B is the ratio of the aerosol backscatter coefficient to that of the background molecular scattering; it is a surrogate for passive scalar concentration. Lidar remote sensing is a time-of-flight technique that uses laser radiation backscattered from atmospheric particulates to obtain range-resolved backscatter measurement fields. The lasers operated at the fundamental wavelength of 1064 nm, suited for the detection of particles with diameter of the order of 1 μm and had a pulse repetition rate of 20 Hz. B was measured continuously in a 2-D vertical planar section.

We analyze ground-based and airborne data sets from B-value of aerosol and cirrus cloud cases (the latter indicated with asterixes; only optically thin clouds can be analyzed due to the extinction of the beam); Langley0807 and Langley0808 are data sets acquired during PACIFIC 2001 in Langley, BC on August 7, 8 with resolution of 3 m, 1 s (roughly 300×5000 points each). Egbert 0530*, 0602, 0603 and 0616* are CARE 2003 data acquired in Egbert, Ontario on 30 May, 02 (the plume of Siberian forest fire), 03 and 16 June (roughly 1000×800 points, except 0530 which was 900×11400). Pacific 0815t6, 0815t8, 0815t10, 0815t18, 0815t22, 0814t5, 0814t7, 0814t9, 0814t17 and 0814t20 are vertical cross-sections from PACIFIC 2001 airborne lidar platform experiments acquired in the Lower Fraser Valley, BC on 14 and 15 (roughly 500×800 points each). We also used 7 (z, t) data sets acquired from RASCAL (Environment Canada's mobile lidar facility [40]) in Windsor, ON during the Border Air Quality Strategy (BAQS) 2004 experimental campaign. These data sets have resolution of 3 m in vertical and of 1 s in time. They represent turbulence in the boundary layer (typical altitudes ~200 to ~1300 m).

In order to justify the statement that B is a good surrogate for passive scalar density, consider Fig. 1 which presents a typical lidar picture. It allows one to make a rough estimate of the apparent vertical wind from the tangent of the cloud structure. In this particular case 45° lines correspond to ~10 cm/s. This speed is much

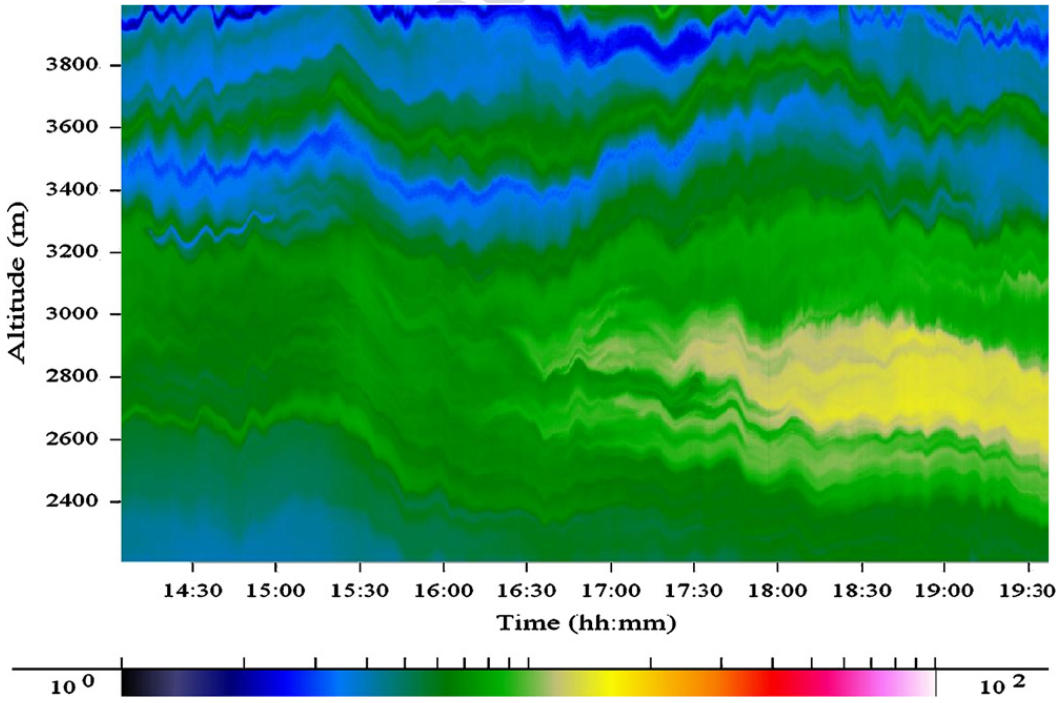

Fig. 1. (Color online) This is the Egbert0603 data taken on 3 June 2003. The scale on the bottom is a logarithmic color scale: darker is for smaller backscatter (aerosol density surrogate), lighter is for larger backscatter. In this panel, the vertical extent is 1.82 km and the duration is 19,440 s. The time resolution is 30.0 s and the vertical resolution is 3.746 m. There is no saturated signal and there is high sensitivity to low signal return.

greater than typical sedimentation rates for particles of the size of 1 μm, which is of the order 0.05 cm/s (more than 100 times smaller).

5. The qualitative analysis

By examining temporal spectra $E(\omega)$, we found no experimental data sets containing a clear break with (i.e. with more than one regime). Overall, we found three cases with $\beta_\tau \approx 2$, the others had $\beta_\tau \approx 5/3$ (see Fig. 2). We also found good agreement between experimental vertical spectra $E(k_z)$ and Bolgiano–Obukhov power law $k_z^{-11/5}$ over wide ranges of scale. The only exception was in some cases where over a limited high wave number range over which we observed $E(k_z) \approx k_z^{-11/5-2}$. This may plausibly be explained by beam attenuation and the post-processing, which attempts to remove it via an attenuation correction. Since the correction is obtained by summing the attenuation coefficients along vertical rays this order 1 integration can readily increase the vertical scaling exponent in real space by 1: $H' = H+1$. For spectral scaling exponent at small k_z we have $\beta' = 2H'+1 = 2H+3 = \beta+2$ i.e. $k_z^{-21/5}$ instead of $k_z^{-11/5}$. Thus, summing the signals over a short range of scales may lead to the observed.

The functional form (22) suggests the use of the following nonlinear transformation of variables (in analogy with real space; see [16]):

$$k_z' = |k_z|^{1/h}\mathrm{sgn}(k_z); \quad \omega' = \omega \tag{25}$$

in the (k_z, ω) domain, or:

$$k_z' = |k_z|^{1/H_z}\mathrm{sgn}(k_z); \quad k_x' = k_x \tag{26}$$

in (k_x, k_z) domain.

Thus, the factorization property (22) implies that contour plots of $P(k_z'\omega')$ should give contours of the same shape at any scale (the shape only depends on the polar angle). For horizontal and vertical wind dominated vertical-time and vertical–horizontal cross-sections (see Figs. 3(a)–(c) respectively), we can clearly see that the large and small contours after transformation (but not before) have the same shape (only depend on

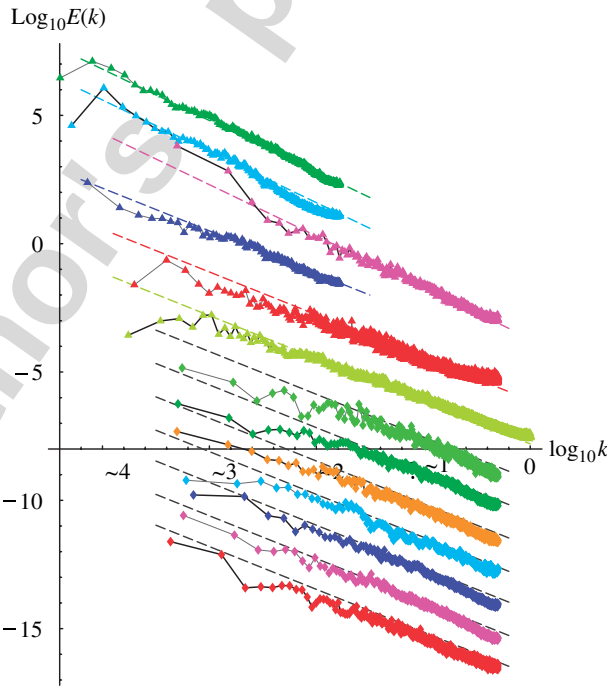

Fig. 2. Temporal spectra. The top 3 curves have reference lines with $\beta_\tau \approx 2$, all the others have $\beta_\tau \approx 5/3$. The top 6 data sets (triangles) were acquired during Pacific 2001 and Egbert 2003 experimental campaigns. The bottom 7 sets were acquired during BAQS 2004 (Windsor) experimental campaign. The spectra are displaced in the vertical for clarity.

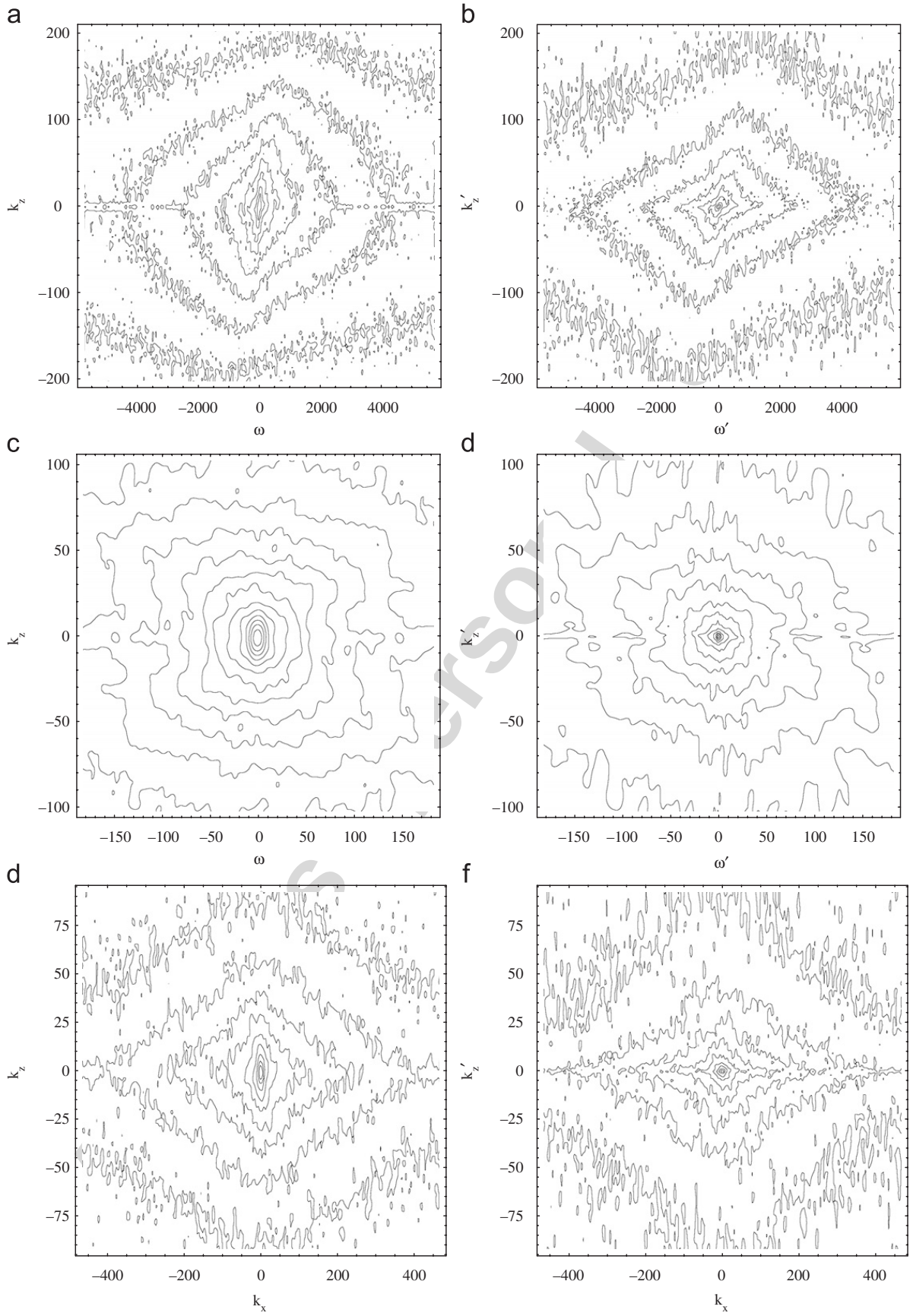

Fig. 3. (a) Contour plots of $\log(P(k_z,\omega))$ (left picture, before nonlinear transformation) and $(P(k'_z,\omega'))$ (after transformation) for Egbert 0530 data set (the case of horizontal wind "domination"). The spectra are smoothed with a radius 4 gaussian smoother in Fourier space; (b) Same as 2a but for Egbert 0603 data set (the case of vertical wind domination). The spectra are smoothed with a radius 6 Gaussian smoother in Fourier space; (c) Same as 2a but for Pacific 2001 0815t22 data set ((x, z) cross section). The spectra are smoothed with a radius 4 Gaussian smoother in Fourier space.

polar angle). The spectra shown in Fig. 3 have a central symmetry; this is a consequence of the definition of the spectrum.

In order to see the anisotropic scale invariance more clearly—and to visually verify that the correct exponents are not far from the theoretical ones—we constructed Fig. 4(a), (b) which shows two successive "zooms" of factor 4 (left to right) on increasingly stratified spaces (lower and lower H_z, bottom to top). Contours at the second row of plots in Fig. 4(a) ($H_z = 5/9$) look pretty much the same as well as contours in

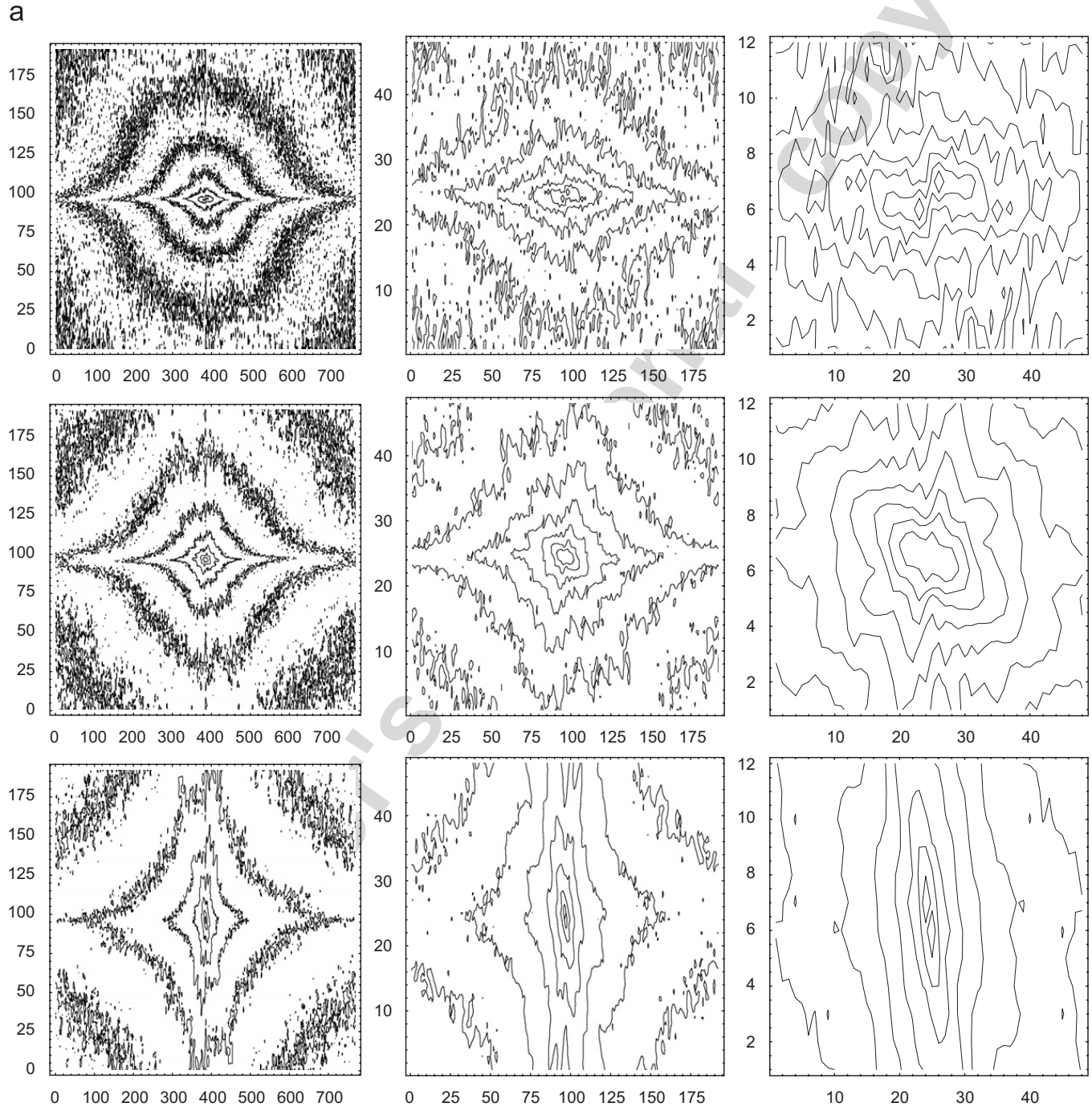

Fig. 4. (a) Contour plots of $(P(k'_x, k'_z))$ for Pacific 0815t8 (x, z) cross section transformed with $H_z = 1/3$ (quasi linear gravity waves), 5/9 (anisotropic 29/9-D model) and 1 (isotropic 3-D turbulence) (from top to bottom) and zoomed with factors 1, 4 and 16 (from left to right); (b) Contour plots of $\log(P(k'_z, \omega'))$ for Egbert 0602 (z, t) cross section transformed with different values of H_z/H_t corresponding to different theoretical approaches: 1/2 (top; gravity waves), 5/6 (middle; anisotropic 29/9-D model) and 1 (bottom; isotropic 3-D turbulence) and zoomed with factors of 1, 4 and 16 (from left to right).

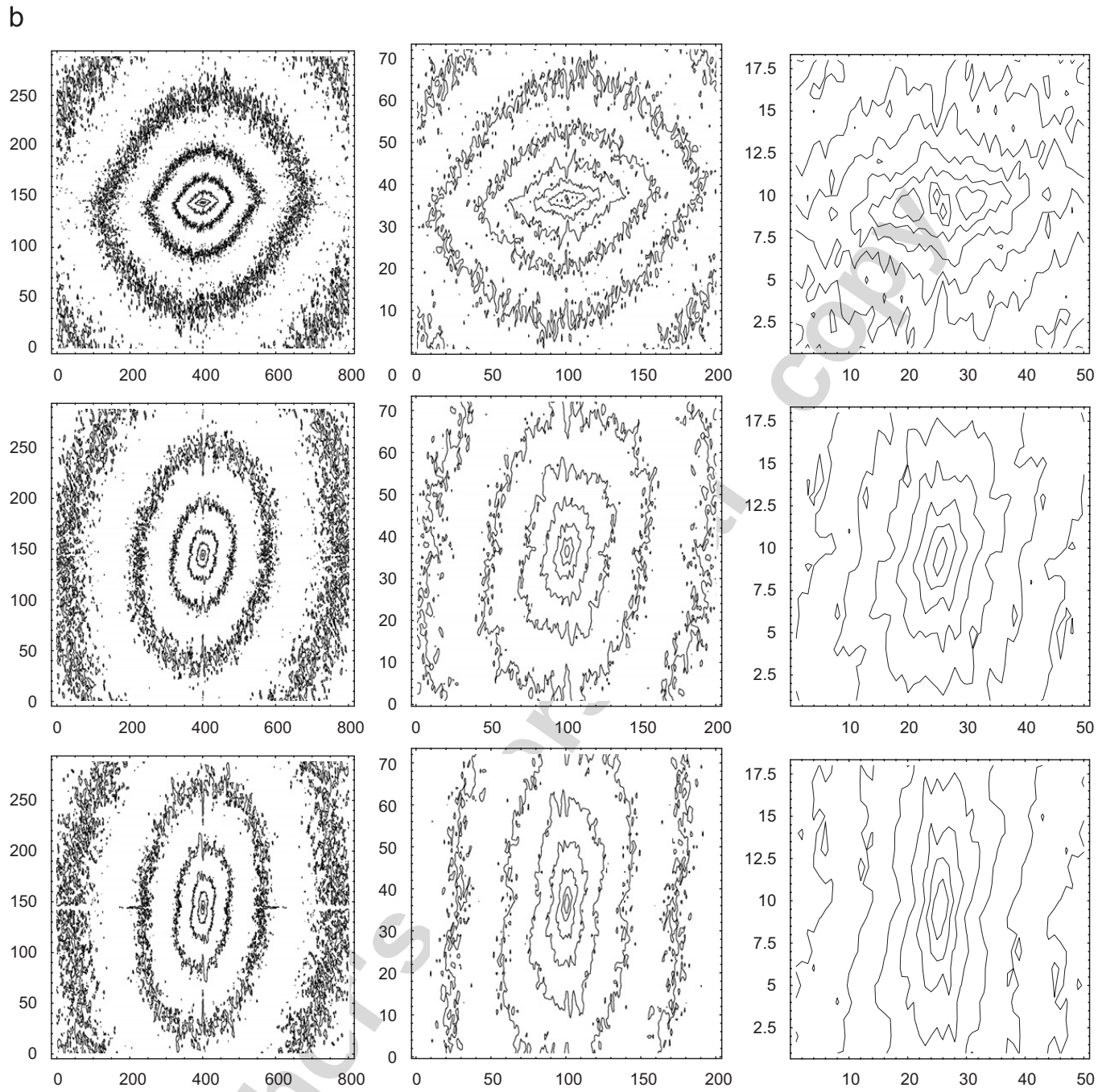

Fig. 4. (*Continued*)

the second row of Fig. 4(b) ($h = 5/6$; the transformation (26) is used, the scaling exponent is $s' = \beta_\tau + H_z/H_t = 17/6$). The last row in both cases corresponds to the isotropic case. The scale independence of the anisotropy contours after the nonlinear transformation with correct (theoretical) power of transformation (but scale *dependence* before) is convincing evidence that Eqs. (25), (26) are valid. In order to see the structure clearly it was necessary to smooth the spectra. Figs. 4(a), (b) are made using a smoothing technique that smoothes along a radial (fixed Fourier space angle θ') and which exploits the isotropic scaling properties of the field in the primed space [41]:

$$\overline{P}(k', \theta') = \frac{1}{2n+1} \sum_{j=-n}^{n} \lambda^{js} P(\lambda^j k', \theta'). \tag{27}$$

Here, we produce $\bar{P}$ smoothing over a factor of roughly 1/4 smaller to 4 larger scales using $n = 11$ and $\lambda = 1.14$. In Fig. 4(a), comparing the left and right contours for $H_z = 1/3$ we can see that they become more "squashed" horizontally while for bottom row ($H_z = 1$) the squashing makes them more and more vertically aligned. The $H_z = 5/9$ (middle) is roughly unchanged. Similarly, in Fig. 4(b), moving from left to right (zooming) we see that the top row is too flattened while the bottom row is too vertically aligned.

Additional evidence for the theoretical exponents and behavior is provided by Fig. 5(a), (b), which presents direct evidence of accuracy of Eq. (22), hence by implication Eq. (10) is valid for all $(\Delta z, \Delta t)$. Note that no single direction θ' in Fig. 5 coincides with the axes ω' or k'_x, k'_z, thus none of the curves represents usual 1-D temporal or space analysis.

6. Quantitative analysis

The above analyses provide qualitative tests of theoretical exponents but not empirical estimates of their values. In order to quantify them—i.e. to estimate $h = H_z$ ((x, z) section) and $h = H_z/H_t$ ((z, t) section) we used a variation on the "Scale Invariant Generator" (SIG) technique developed earlier [41,42]. This technique estimates h by minimizing the differences between the zoomed $\overline{P}(\lambda \underline{k}')$ and original spectra $\overline{P}(\underline{k}')$ of Fig. 4. This difference is quantified by the following error function $E^2 = \overline{\left[\log(\overline{P}(\lambda \underline{k}')\lambda^s) - \log(\overline{P}(\underline{k}'))\right]^2}$ where the factor λ^s ($s = \beta_\tau H_{t,\,eff} + H_z$) takes into account the scaling $\bar{P} \propto k^{-s}$. β is the 1-D spectral exponent in the horizontal (temporal) direction; as above, the overbar means averaging along a radial in the space (k'_x, k'_z) or (k'_z, ω') and over all radials (to cover the whole space). Before performing the analysis it was important to remove high frequencies and/or wave numbers affected by measurement noise.

In order to verify this technique we applied it to various anisotropic multifractal simulations with known parameters. We found good agreement between the original parameters of the simulations and those ones calculated with technique described above with the only exception that this technique systematically slightly underestimates stratification exponent (by about 0.02–0.03). This is a (at least) partial explanation of the underestimation of the stratification exponent found for the real data we shall show below.

The dependencies of E^2 on $h = H_z$, $(h = H_z/H_t)$ as well as their quadratic fits are presented on the Figs. 5–7. A quadratic fit near the minimum was used to accurately obtain the position of minimum of E^2 as a function of h. The results are given by Tables 1 and 2 (Fig. 8).

The mean value of the "wind dominated" cases 4–6 is $h = H_z = 0.57 \pm 0.05$, the mean value of the pure temporal cases 1–3 is $h = H_z/H_t = 0.79 \pm 0.09$. Using $H_t = 1$ or 2/3 we can see that the theoretical values (5/9, 5/6) are within the confidence intervals in both cases. The mean over the 10 (x, z) cross sections cases 7–16 is $H_z = 0.50 \pm 0.04$. In all cases we note a small systematic underestimate of H_z.

In order to estimate H_t from the empirically determined ratio H_z/H_t, we need an estimate of H_z. Using the empirical value $H_z = 0.50$ we find $H_t = 0.63 \pm 0.12$. Alternatively, if we assume the theoretical value $H_z = 5/9$, we obtain $H_t = 0.70 \pm 0.08$; both estimates are near the value 2/3. Finally, we can calculate the space-time dimension of turbulent motions D_{st}, which is given by the following expression:

$$D_{st,eff} = Tr(G_{eff}) = 1 + 1 + H_z + H_{t,eff}.$$

Using the empirical $H_z = 0.50$ to estimate H_t we obtain $D_{st,eff} = 3.13 \pm 0.16$ or using the theoretical $H_z = 5/9$ we obtain alternatively $D_{st,eff} = 3.25 \pm 0.08$. It is important to note that these estimates of the "effective" elliptical dimension are valid for both cases of horizontal and vertical wind domination (if we accept that the pure temporal development is never dominant over the observed scale range). Horizontal wind does not change the trace of the generator G while vertical wind with temporal scaling does.

Although the underestimate in H_z with respect to the 5/9 value is small and nearly within the one standard deviation error bar, it may be significant. A possible explanation for the slightly low H_z value is that at least for the higher altitudes (>4–5 km) that the value of H_v may increase from 3/5 to ≈ 0.75 ([45] using state-of-the-art dropsondes to measure vertical profiles of horizontal wind). If this is the case, then a

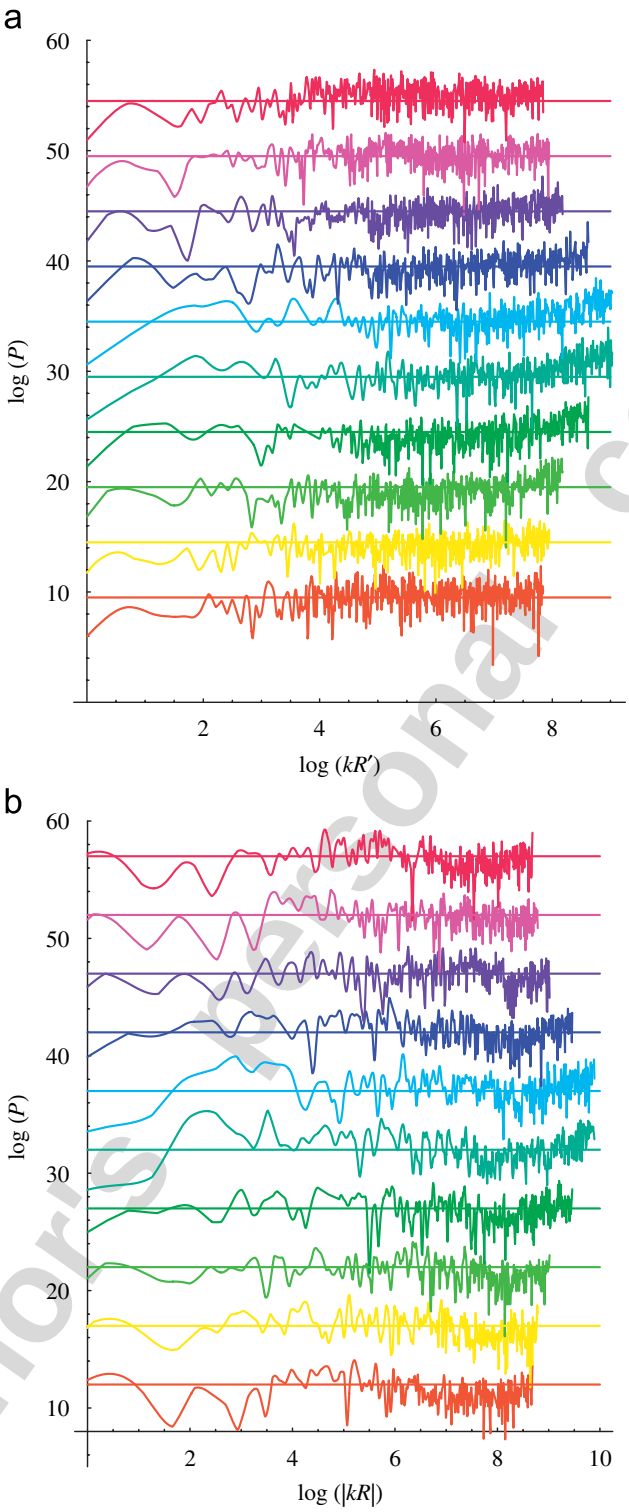

Fig. 5. 1-D dependences of $k_R^s P(k_R, \theta')$ (i.e. the spectrum compensated by k_R^s) on k_R along different rays $\theta' = \pi/20$, $3\pi/20$,…, $19\pi/20$ (top to bottom) the theory is validated when the lines are flat. This is a direct test of Eq. (22) in arbitrary directions in k' space. Dependences for different directions are equally offset for clarity. Bottom lines correspond to low values of θ'; straight lines are reference lines parallel to horizontal axis; (a) Langley 0808 dataset (case of horizontal wind domination, $s = 20/9$), (b) Egbert 0603 dataset (case of vertical wind domination, $s = 1.89$).

pure $H_z = 0.75$ regime would yield $H_z = 0.44$ (not 5/9), quite close to some of the values in Table 2. Values intermediate between 0.44 and 0.55 would result from averaging over thick atmospheric layers including both regimes.

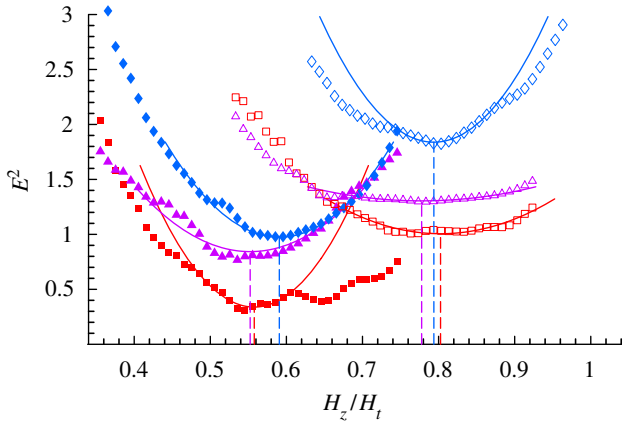

Fig. 6. Error E^2 as a function of H_z and the quadratic fit near the minimum for (z,t) data sets. Filled dots represent wind "dominated" cases, non-filled–cases with pure temporal development. (Red filled boxes)—E0530, (violet filled triangles)—E0616, (blue filled diamonds)—L0808, (red boxes)—E0602, (violet triangle)—E0603, (blue diamonds)—L0807. The curves are offset in the vertical for clarity. The vertical dashed lines indicate minima of fits. Their values are given in Table 1.

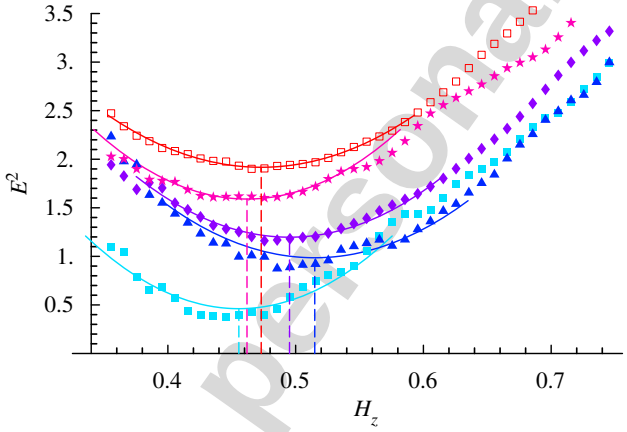

Fig. 7. Same as 5 but for (x, z) data sets: Pacific 2001 0814. (Light blue boxes)—0814t5, (blue triangles)—0814t7, (violet diamonds)—0814t9, (pink stars)—0814t17, (red unfilled boxes)—0814t20.

Table 1
This compares the RMS exponents for various (z, t) data sets discussed in the text

Data set	Type of cloud	Resolution (vertical-time)	H_z/H_t^*	Dilation factor λ
1. Egbert 0602[a]	Cirrus	3.75 m by 30.0 s	0.803 ± 0.088	16
2. Egbert 0603[a]	Aerosol	3.75 m by 30.0 s	0.778 ± 0.10	8
3. Langley 0807[a]	Aerosol	3.0 m by 1.0 s	0.794 ± 0.075	16
Mean, vertical wind domination data sets			0.79 ± 0.09	
4. Egbert 0530[b]	Cirrus	3.75 m by 0.5 s	0.558 ± 0.085	16
5. Egbert 0616[b]	Cirrus	3.75 m by 30.0 s	0.552 ± 0.037	16
6. Langley 0808[b]	Aerosol	3.0 m by 1.0 s	0.591 ± 0.021	16
Mean, horizontal wind dominated data sets			0.57 ± 0.05	

The dilation factor used in the estimates was the largest compatible with the data (recall that we require a range of scale of factor $\geqslant 40$ after the zoom in order to make a reliable comparison) and varies slightly as indicated. The values and errors are from the error functions graphed in Fig. 6.

[a]Horizontal wind dominates theory is $5/9 \approx 0.555\ldots$

[b]Pure temporal development, theory is $5/6 \approx 0.833\ldots$

Table 2
Same as Table 1 but for (x, z) cross-sections

Data set	H_z	Dilation Factor λ
7. P 0814t5	0.454 ± 0.053	16
8. P 0814t7	0.515 ± 0.033	16
9. P 0814t9	0.495 ± 0.034	16
10. P 0814t17	0.462 ± 0.068	8
11. P 0814t20	0.473 ± 0.019	8
12. P 0815t6	0.538 ± 0.060	16
13. P 0815t8	0.541 ± 0.034	16
14. P 0815t10	0.482 ± 0.035	16
15. P 0815t18	0.521 ± 0.034	8
16. P 0815t22	0.514 ± 0.033	16
Mean	0.50 ± 0.04	

All data sets represent aerosol clouds and have resolution 96 m (horizontal) by 3 m (vertical). The values and errors are from the graphs in Figs. 7, 8.

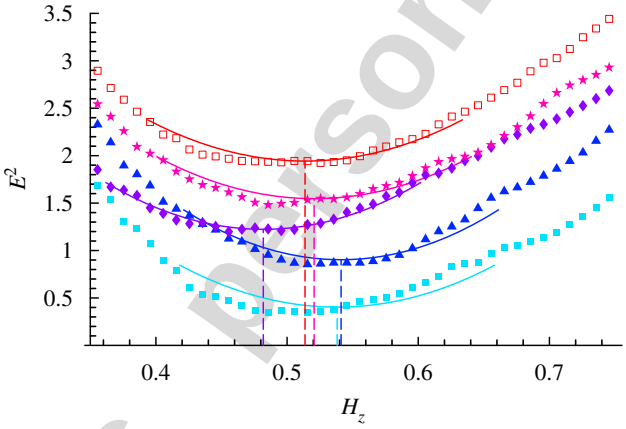

Fig. 8. Same as 5 but for (x, z) Pacific 2001 0815 data sets. (Light blue boxes)—0815t6, (blue triangles)—0815t8, (violet diamonds)—0815t10, (pink stars)—0815t18, (red unfilled boxes)—0815t22.

7. Conclusions

One of the most fundamental aspects of atmospheric turbulence is its space-time stratification. Over the last 20 years the evidence has accumulated that it is scaling over wide ranges of space-time scales. Indeed, the main competing theories are the scaling quasi-linear gravity wave theories and the anisotropic generalization of Bolgiano–Obukhov convectively driven turbulence. In the horizontal and vertical directions these theories predict spectral exponents 5/3, 3 and 5/3, 11/5, respectively; the scaling stratifications implied by these models can be characterized by the "elliptical dimensions" $D_s = 7/3$ and $D_s = 23/9$, respectively. As is often the case, key breakthroughs come with advent of new technologies; in this case, state-of-the-art lidar backscatter data from passive scalars which yielded the estimate [15] $D_s = 2.55 \pm 0.02$, thus ruling out the competing quasi-linear gravity wave theories. At about the same time, scaling analyses of aircraft trajectories revealed that not only can they be fractal, but that the fractality systematically bias the turbulence exponents and—if the trajectories are not perfectly flat—can introduce spurious length scales and even spurious exponents [23,43].

In the absence of overall advection, the $D_s = 23/9$ model of spatial stratification implies that space-time is scaling with exponent $D_{st} = 29/9$. However, when advection is taken into account, it is found to introduce off-diagonal elements in the generator of the group of scaling changing operators so that space-time cross-sections become more complicated than vertical–horizontal cross-sections. Although if one uses appropriate anisotropic notions of scale, there will only be a unique scaling behavior, if one considers time series and uses Δt or frequency ω (i.e. conventional times and frequencies) we find that there are three different temporal scaling regimes corresponding to dominance by horizontal advection, pure temporal development and vertical advection. Viewed in this way, this is a "cross-over" scaling phenomena: the three scalings are always present but at a given scale—depending on the local values of the turbulent fluxes and horizontal and vertical winds—one will be dominant.

Analyzing the effects of advection more closely we found that although gradients in the horizontal wind are scaling, there may still be a roughly uniform advection across our experimental region. However, the vertical wind is quite different; its space-time averages have non-trivial scaling properties such that averaging it over larger and larger scales tends to reduce it. Taking this scaling into account, we find that the vertical advection exponent (which is a consequence of both vertical stratification and the non-trivial scaling of the vertical velocity) is actually quantitatively very close to the temporal scaling exponent; both lead to $\beta_\tau \approx 2$. At the same time, because of the advection effects of smaller eddies by planetary scale ones, pure temporal development—at least for scales below the eddy turn-over time for the largest eddy (about 2 weeks)—is unlikely to be observed. We therefore argue that the observed exponents $\beta_\tau \approx 5/3, 2$ correspond to horizontal or vertical wind domination. We can reduce the problem to advection with constant horizontal wind and use an "effective" generator G_{eff} temporal stratification exponent $H_{t,eff}$ which is determined by the scaling properties of the vertical wind.

Building on the earlier (x, z) (vertical cross-section) lidar work, we test these predictions using passive scalar surrogates of aerosol and cirrus clouds from thirteen ground based lidar cross sections (vertical-time) and ten airborne lidar cross sections (vertical–horizontal), thereby directly accessing both vertical and time (or horizontal and vertical) information.

In order to estimate scaling space-time stratification for density fluctuations, we developed new anisotropic scaling analysis technique (ASAT) based on nonlinear coordinate (wave numbers and frequency in Fourier space) transformations. The idea is to use a nonlinear coordinate transformation to transform the data into an isotropic space so that the spectra become self-similar. Since the spectra in the new space is self-similar, this allows us to visually validate the theory as well as to quantitatively estimate the stratification exponents.

Our findings of the stratification exponents are based on the analysis in all wave numbers and frequency directions for space-time scales ranging over roughly 3 orders of magnitude. Using the ASAT technique, we obtained the estimate of the vertical stratification exponent from vertical–horizontal cross sections close to its theoretical value of 5/9: $H_z = 0.50 \pm 0.04$; i.e. a little smaller than previous estimates based on (real space) first-order structure functions, but still within the one standard deviation error bars. The ratio of the stratification exponents $H_z/H_{t,eff}$ for the cases of the horizontal wind domination ($H_{t,eff} = 1$) is also close to the theoretically predicted value (5/9), we found: $H_z/H_{t,eff} = 0.57 \pm 0.05$. For the cases of vertical wind domination, we have $H_z/H_{t,eff} = 0.79 \pm 0.09$ and $H_{t,eff} = 0.70 \pm 0.08$. Ignoring intermittency, this implies that the temporal scaling exponent of the vertical wind is $H_w = H_z/H_{t,eff} - 1 = -0.2 \pm 0.1$. In an accompanying series of papers, [16,23,44] we show that this result is fully compatible with numerous existing (sonde, aircraft) data analyses, we show how to make the corresponding multifractal models including extensions to turbulence/wave models which although close to the observed wave phenomenology are highly nonlinear consequences of the anisotropic scaling rather than quasi-linear phenomenon predicted by linear perturbation theory of the turbulent atmospheric equations. Finally, since horizontal advection does not change the trace of the generator G the effective dimension of space-time is $D_{st,eff} = 2 + H_z + H_{t,eff} = 3.25 \pm 0.1$ or 3.13 ± 0.16 depending on the method of estimation in the two cases.

The classical turbulence approaches to atmospheric dynamics proceed by first postulating isotropy and then scaling. Since the phenomena are highly stratified in both space and space-time, this greatly reduces the range over which any given theory is applicable. In addition in order to explain the dynamics over the enormous range of dynamically important scales, it requires the elaboration of a hierarchy of (often ad hoc) models including their non-trivial interlinkages. In contrast, modern data has shown that in spite of extreme

anisotropies, that the space-time scaling of many turbulent atmospheric fields can nevertheless be remarkably well respected over huge ranges of scale. By showing that the same anisotropic framework (GSI) is adequate for both spatial and space-time stratification, we vastly extend the range of scales over which turbulence theory can be applied, and open up the possibility that one day all meteorological phenomena will be satisfyingly treated as anisotropic turbulent phenomena. This implies the possibility of developing new families of (anisotropic, multifractal) models—including some with wave-like behaviors (Lovejoy et al., 2007)—as well as new (stochastic) approaches to meteorological forecasting.

Acknowledgments

The authors also acknowledge the Center for Atmospheric Research Experiments of Environment Canada for the close collaboration during this project and in particular the support of M. Travis. We also acknowledge the Canadian Foundation for Climate and Atmospheric Sciences for financial support.

References

[1] I. Arad, B. Dhruva, S. Kurien, V.S. L'vov, I. Procaccia, K.R. Sreenivasan, Phys. Rev. Lett. 81 (1998) 5330.
[2] I. Arad, L. Biferale, I. Mazzitelli, I. Procaccia, Phys. Rev. E 82 (1999) 5040.
[3] I. Arad, V.S. L'vov, I. Procaccia, Phys. Rev. E 59 (1999) 6753.
[4] S. Kurien, V.S. L'vov, I. Procaccia, K.R. Sreenivasan, Phys. Rev. E 61 (2000) 407.
[5] V.S. L'vov, I. Procaccia, V. Tiberkevich, Phys. Rev. E 67 (2003) 026312.
[6] D. Schertzer, S. Lovejoy, Physico-chem. Hydrodyn. J. 6 (1985) 623.
[7] D. Schertzer, S. Lovejoy, in: B. Launder (Ed.), Turbulent Shear Flow 4, Springer, 1985, p. 7.
[8] P. Bartello, J. Atmos. Sci. 52 (1995) 4410.
[9] A.L. Fairhall, B. Dhruva, V.S. L'vov, I. Procaccia, K.R. Sreenivasan, Phys. Rev. Lett. 79 (1997) 3174.
[10] J.L. Lumley, Phys. Fluids 10 (1967) 1405.
[11] J.C. Wyngaard, O.R. Cote, J.R. Quar, Met. Soc. 98 (1972) 590.
[12] T. Ishihara, K. Yoshida, Y. Kaneda, Phys. Rev. Lett. 88 (2002) 154501.
[13] Y. Chigirinskaya, D. Schertzer, S. Lovejoy, et al., Nonlinear Process. Geophys. 1 (1994) 105.
[14] A. Lazarev, D. Schertzer, S. Lovejoy, et al., Nonlinear Process. Geophys. 1 (1994) 115.
[15] M. Lilley, S. Lovejoy, K. Strawbridge, D. Schertzer, Phys. Rev. E 70 (2004) 036307.
[16] A. Radkevich, S. Lovejoy, K.B. Strawbridge, et al., Quart. J. R. Meteor. Soc. (2006), submitted for publication.
[17] E. Inoue, J. Met. Soc. Jpn 29 (1951) 32.
[18] L.D. Landau, E.M. Lifshitz, Fluid Mechanics, Pergamon, London, England, 1959.
[19] D. Schertzer, M. Larchevesque, J. Duan, S. Lovejoy, Generalized Stable Multivariate Distributions and Anisotropic Dilations, IMA preprint # 1666, Institute For Mathematics And its Applications, University of Minnesota.
[20] D. Schertzer, S. Lovejoy, F. Schmitt, et al., Fractals 5 (1997) 427.
[21] D. Schertzer, S. Lovejoy, F. Schmitt, et al., in: University Department of Energy (Ed.), Seventh Atmos. Rad. Meas. (ARM) meeting, San Antonio, 1998, p. 327.
[22] H. Tennekes, J. Fluid. Mech. 67 (1975) 561.
[23] S. Lovejoy, D. Schertzer, M. Lilley, et al., Quart. J. R. Meteor. Soc. (2005), submitted for publication.
[24] A.O. Scheffler, C.H. Liu, Radio Sci. 20 (1985) 1309.
[25] B.B. Balsley, R. Garello, Radio Sci. 20 (1985) 1355.
[26] D.C. Fritts, T. Tsuda, T.E. VanZandt, S.A. Smith, T. Sato, S. Fukao, S. Kato, J. Atmos. Sci 47 (1990) 51.
[27] M.L. Larsen, M.C. Kelly, K.S. Gage, J. Atmos. Sci 39 (1982) 1035.
[28] B.B. Balsley, D.A. Carter, Geophys. Res. Lett. 9 (1982) 465.
[29] R.J. Sica, A.T. Russell, J. Atmos. Sci. 56 (1999) 1308.
[30] C.E. Meek, I.M. Reid, A.H. Manson, Radio Sci. 20 (1985) 1383.
[31] C.S. Gardner, D.G. Voelz, J. Geophys. Res 92 (1987) 4673.
[32] K.H. Kwon, C.S. Gardner, S.K. Avery, J.P. Avery, J. Geophys. Res 95 (1990) 13737.
[33] T.J. Beatty, C.A. Hostetler, C.S. Gardner, J. Atmos. Sci. 49 (1992) 477.
[34] S. Lovejoy, D. Schertzer, Multifractal analysis techniques and rain and cloud fields from 10–3 to 106 m. In: D. Schertzer, S. Lovejoy (Eds.), Scaling, Fractals and Non-linear Variability in Geophysics, Kluwer, Dordrecht, 1991, pp. 111–144.
[35] V. Venugopal, E. Foufoula-Georgiou, V. Sapozhnikov, J. Geophys. Res. 104 (1999) 31599.
[36] L. Skrbek, J.J. Niemela, K.R. Sreenivasan, R.J. Donnelly, Phys. Rev. E 66 (2002) 036303.
[37] J.J. Niemela, L. Skrbek, K.R. Sreenivasan, R.J. Donnelly, Nature 404 (2000) 837.
[38] S. Ashkenazi, V. Steinberg, Phys. Rev. Lett. 83 (1999) 4760.
[39] X.-D. Shang, K.-Q. Xia, Phys. Rev. E 64 (2001) 065301.

[40] K.B. Strawbridge, B.J. Snyder, Atmos. Environ. 38 (2004) 5873.
[41] G.M. Lewis, D. Schertzer, S. Lovejoy, S. Pecknold, Comput. Geosci. 25 (1999) 963.
[42] Q. Cheng, Math. Geol. 36 (2004) 345.
[43] S. Lovejoy, D. Schertzer, A.F. Tuck, Phys. Rev. E 70 (2004) 036306.
[44] M. Lilley, S. Lovejoy, K. Strawbridge, D. Schertzer, A. Radkevitch, Quart. J. Roy. Meteor. Soc., (2005), submitted for publication.
[45] S. Lovejoy, A. Tuck, S. Hovde, D. Schertzer, Geophys. Resear. Lett. (in press).